Application of ANFIS Power Control for Downlink CDMA-Based LMDS Systems

Ze-Shin Lee, Mu-King Tsay, and Chien-Hsing Liao

Rain attenuation and intercell interference are two crucial factors in the performance of broadband wireless access networks such as local multipoint distribution systems (LMDS) operating at frequencies above 20 GHz. Power control can enhance the performance of downlink CDMA-based LMDS systems by reducing intercell interference under clear sky conditions; however, it may damage system performance under rainy conditions. To ensure robust operation under both clear sky and rainy conditions, we propose a novel power-control scheme which applies an adaptive neuro-fuzzy inference system (ANFIS) for downlink CDMA-based LMDS systems. In the proposed system, the rain rate and the number of users are two inputs of the fuzzy inference system, and output is defined as channel quality, which is applied in the power control scheme to adjust the power control region. Moreover, ITU-R P.530 is employed to estimate the rain attenuation. The influence of the rain rate and the number of users on the distance-based power control (DBPC) scheme is included in the simulation model as the training database. Simulation results indicate that the proposed scheme improves the throughput of the DBPC scheme.

Keywords: Adaptive neuro-fuzzy inference systems, power control, intercell interference, LMDS, rain attenuation.

Manuscript received May 21, 2008; revised Nov. 27, 2008; accepted Feb. 10, 2009.

Ze-Shin Lee (phone: 886 3 4515104, email: zeshin.lee@msa.hinet.net) was with the Department of Communication Engineering, National Central University, Taoyuan, Taiwan, and is currently with the Department of Electrical Engineering, Minghsin University of Science and Technology (MUST), Hsinchu, Taiwan.

Mu-King Tsay (email: tsaymk@ce.ncu.edu.tw) is with the Department of Communication Engineering, National Central University, Taoyuan, Taiwan.

Chien-Hsing Liao (email: jason_arpon@so-net.net.tw) was with the Department of Communication Engineering, National Central University, Taiwan, and is currently with Chung-Shan Institute of Science and Technology (CSIST), Taiwan.

I. Introduction

Local multipoint distribution service (LMDS), a fixed broadband wireless technology, is employed to provide multimedia communication services to subscribers in fixed locations through millimeter wave transmissions in a range from 20 GHz to 50 GHz. As a digital cellular point-to-multipoint (PMP) distribution system, LMDS offers a wireless access method for broadband interactive services and provides a wide bandwidth ranging from 0.1 GHz to 2 GHz [1]-[3].

In current standards, time-division multiple access (TDMA) is employed as a multiple access scheme in downlink LMDS systems. The code-division multiple-access (CDMA) scheme has become popular because it is able to support a large number of simultaneous users. The CDMA scheme has greater bandwidth efficiency and multiple access capability than TDMA [4]. Previous studies have verified that CDMA-based LMDS systems have a higher immunity to interference than TDMA-based ones for uplinks [5]-[8], and the opposite condition exists in downlinks, where users with highly directional antennas have higher worst-case interference in CDMA-based LMDS systems than in TDMA-based LMDS systems. In CDMA-based LMDS systems, in which all users share the same frequency band in a cell, the intercell interference of the system is strongly dependent on the number of users in the interfering cell sectors. In the cellular environment, the existing intercell interference reduces the signal-to-interference ratio (SIR). Due to the high operating frequency, LMDS systems suffer from a requirement for a clear line-of-sight (LOS) link between the base station (BS) and the terminal station (TS) [9], [10]. The LOS confinement and large propagation losses, particularly free-space loss and rain attenuation, limit the coverage area of LMDS systems. The

effect of rain attenuation on LMDS systems has been widely investigated and published. Both theoretical and experimental analysis demonstrate that rain attenuation highly depends on the rain rate and drop-size distribution [8], [11], [12].

Power control is essential in CDMA schemes to compensate for radio channel fading [13]. With an appropriate power control, CDMA-based LMDS systems have a higher capacity than FDMA- or TDMA-based LMDS systems [9]. Because the locations of TSs in LMDS systems are fixed, the downlink power-control implementation is simpler than in mobile systems. Distance-based power control (DBPC), which was proposed by Lee in [14] and further studied by Gejji in [15], is applied to the downlink CDMA-based LMDS systems. In DBPC, the transmitted power is derived directly from the distance between BS and TS, and no feedback is provided to the serving BS. This is easier to implement than closed-loop power control and has no transmitted power delay [14]-[16]. However, these studies gave little attention to the channel environmental condition, that is, rain rate and intercell interference. Under clear sky conditions, the DBPC scheme does indeed improve the system performance by reducing intercell interference, but this is not true under rainy conditions. On the contrary, it may hinder the performance of downlink CDMA-based LMDS systems under rainy conditions. As previously mentioned, rain attenuation and intercell interference critically affect the performance of LMDS systems, and the influence of these two factors on the system is hard to accurately model mathematically for the implementation of a conventional controller.

Fuzzy power control and neural network power control have been demonstrated to improve the system performance for CDMA systems [17]-[19]. The implementation of these two schemes is based on the concept of fuzzy set theory and the experience of expert operators, who can construct a control scheme without a sharp mathematic model. Nevertheless, they suffer from the same disadvantage of requiring parameter model identification. For instance, in fuzzy logic control, the number of membership functions for each input variable must be defined in advance, and this consequently generates a large number of redundant fuzzy control rules, resulting in more complex computation and memory consumption. Recently, the back propagation learning rule has been applied into artificial neural networks. An artificial neural network is a universal learning paradigm for the smooth parameterized model covered in a fuzzy inference system. Consequently, the fuzzy inference system takes linguistic rules from human experts and adapts itself to achieve a desirable performance by means of an input-output database. For instance, Jang proposed the adaptive neuro-fuzzy inference system (ANFIS) scheme, which combines a fuzzy inference system with neural networks and applies a hybrid learning rule. The resulting system inherits the advantages of both neural networks and fuzzy systems, and avoids the disadvantages of these two schemes [20]. It is widely used in fuzzy control systems and pattern identification systems.

To ensure robust operation under both clear sky and rainy conditions, we propose a novel power control scheme applying ANFIS to the DBPC scheme to compensate for the attenuation which results from rain and the propagation path. The scheme is intended to enhance the performance of downlink CDMA-based LMDS systems. Rain attenuation is one of the major causes of unavailability for radio communication operating at high frequency bands. It is necessary to apply the dynamics and spatial variation of rain intensities to estimate the attenuation with accuracy. To explain the rain attenuation and the average path effect for the spatial structure of the rain rate in a moving rain cell, the spatial resolution measurement field must be large enough. However, for simplicity and without lack of representativeness, this work applies ITU-R P.530 to evaluate the rain attenuation which exceeds 0.01% of the time.

In the proposed ANFIS power control, the rain rate and number of users in the interfering cell sectors are the two inputs of the fuzzy inference system, and one output of the fuzzy inference system is defined as channel quality, which is applied to power control scheme to determine the power control region. The related input data and the coverage ratios of DBPC for the downlink CDMA-based LMDS system are used to create a training database for various associated channel environment conditions and training the ANFIS with the pre-training samples so as to obtain desirable control rules. In this paper, the application of ANFIS power control along with dynamic modulation for downlink CDMA-based LMDS systems will demonstrate that its average throughput is superior to that of DBPC schemes.

The remainder of this paper is organized as follows. The system model and propagation characteristics are described in section II. Section III will briefly describe the basic ANFIS scheme. In section IV, the performance and comparison of the proposed ANFIS power control and DBPC schemes will be described in more detail. Section V concludes this paper.

II. System Model and Propagation Characteristics

The system model and propagation characteristics used in this paper are similar to those which are described in [5], [9], and [10]. In the design of any radio communication system, to obtain a given level of performance, availability, and maximum range, a link budget analysis must be performed to established necessary transmitted power, antenna gains, modulation gains, and so on. The free space loss together with other effects, such

as clear air absorption and rain are the most influential factors. LMDS systems operating at spectral ranges above 20 GHz suffer from the effect of molecular absorption. The effect of propagation on LMDS systems is the same as that of millimeter wave propagation. The main radio propagation of LMDS channels includes path loss, intercell interference, atmospheric conditions, galactic noise, and rain attenuation. The propagation loss on a terrestrial LOS path relative to the free-space loss is the sum of the various contributions. A precise estimation of path loss is hard to obtain, and many path loss models for various transmission environments have been presented. In this work, the following equation is used to express path loss propagation:

$$P_R = P_T \times G_T \times G_R \times (\frac{c}{4\pi f})^{\alpha} \times (\frac{1}{d})^{\alpha}, \qquad (1)$$

where P_R represents the receiving power, P_T is the transmitting power, c=3·10^8 m/s, f is the radio frequency in hertz, α is the path loss exponent and the value range between two and five, d is the distance between the transmitting antenna and the receiving antenna, and G_T and G_R are the gains of the transmitting antenna and the receiving antenna, respectively. In general, the value of α is equal to two for free space propagation. For non-LOS link propagation, the value of α is from three to five, depending on the actual conditions of the service area.

A typical downlink CDMA-based LMDS system model with rectangular cell patterns of a given cell length 2D is illustrated in Fig. 1. The heavy dots represent BSs, squares represent TSs, and the BS is located at the center of each cell. The TSs are distributed randomly within each cell, and each cell is distinctly separated by a solid line. Each cell is further subdivided into four sectors that are equally spaced 90° apart. The dotted lines are the boundaries of each sector. Four sectors are allocated one shared frequency band. "A" symbolizes the frequency band allocated to the cell sectors. A two-layer CDMA concept is embedded in this cellular cell planning. That is, the transmitting signals are first multiplied and spread by a Walsh-Hadamard sequence and then multiplied and spread again by a long pseudo-noise (PN) sequence [21]. The latter operation is purely a scrambling operation, and each subscriber is made unique by using a set of orthogonal sequences. Therefore, no downlink interference should occur between the subscribers within the same cell. Consequently, 4N spreading gain for each cell is available if each fully loaded sector occupying a fixed frequency bandwidth can accommodate up to N subscribers with orthogonal sequence codes. Moreover, since deployments of TSs are fixed in a sector, antennas are designed to be highly directional, and the beamwidth is typically within 2° to 5° of the TS [5]. Therefore, the impact of multipath interference is also avoided by adopting an LOS channel and a highly directional TS antenna [5], [8].

Because a TS is linked to the serving BS by an LOS digital radio link and the beamwidth of the TS antenna is very small, the TS antenna receives interference from the interfering BSs which reuses the same frequency band as that shown in Fig. 1. In analysis of the intercell interference for TSs, we assume that an LOS link exists in the middle of three successive BSs. That is, in addition to the desired BS (BS0), LOS links include the adjacent interfering BSs and the second nearest interfering BSs (BS1, BS2,···, BS8).

As shown in Fig. 1, considering that the five TSs, that is, TS1 to TS5 are placed around the upper-right cell boundary of the BS0 cell, their intercell interference sources come mainly from the adjacent BSs visible to the TS antenna and with the same frequency due to reuse. Therefore, there are five possible BS pairs interfering with the TSs, depending on which is visible to the TS. For LOS microwave and millimeter-wave radio systems, all BSs transmit the same signal power, and the signal attenuation is proportional to the squared propagation distance (α = 2). For example, to calculate the SIR of a TS located between BS0 and TS1, besides receiving the signal from the desired BS, the TS also receives two interfering signals from BS1 and BS2. Here, the other minor intercell interference contributions coming from the other BSs are neglected [5]. The distances from BS0 to BS1 and BS2 are 2D and 4D, respectively. For simplicity and without loss of generality, we suppose that there are K_{scc} uniformly distributed subscribers in each sector. When there is no power control under clear sky conditions, the SIR for the considered TS is expressed as in [10] as

$$\mathrm{SIR} = \left(\frac{K_1}{4N} \left(\frac{d}{2D+d} \right)^2 + \frac{K_2}{4N} \left(\frac{d}{4D+d} \right)^2 \right)^{-1}, \qquad (2)$$

where, d is the distance between the desired BS and the TS;

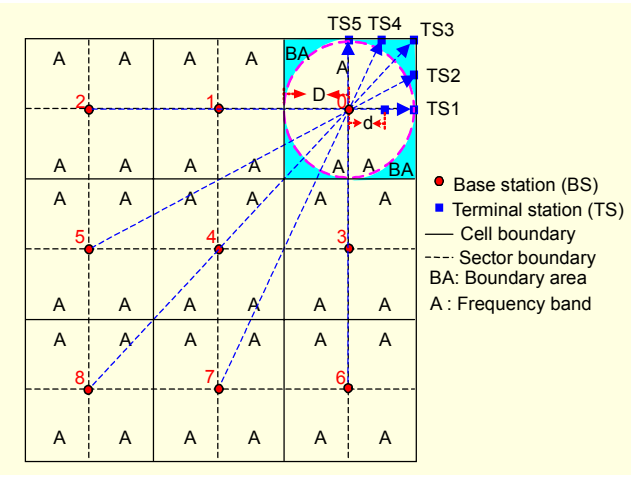

Fig. 1. Cell pattern for downlink CDMA-based LMDS network.

and K_1 and K_2 are the numbers of active interfering users of BS1 and BS2, respectively. Whenever the effects of noise, such as obstruction of buildings, galactic noise, and so on are considered, the SIR plus noise ratio (SINR) is given by

$$\mathrm{SINR} = [(\mathrm{SIR})^{-1} + (\mathrm{SNR})^{-1}]^{-1}, \quad (3)$$

where the signal-to-noise ratio (SNR) can be calculated from the link budget of the LMDS system as given in Table I of [8].

Rainfall restricts communication link distance, limits the use of higher frequencies, and affects system performance [8]. The performance of LMDS systems highly depends on rain attenuation due to the application of high carrier frequencies. To evaluate the effect of rain attenuation on LMDS systems, the ITU-R P.530-10 prediction model can be applied to predict the rain attenuation [22], which is valid throughout the world for frequencies up to 40 GHz and path lengths up to 60 km. The estimate of the path attenuation exceeding 0.01% of the time ($A_{0.01}$) is given by

$$A_{0.01} = a \times R_{0.01}^{b} \times L \times r_{0.01}, \quad (4)$$

$$r_{0.01} = 1/(1 + d/d_0), \quad (5)$$

$$d_0 = 35 \times e^{-0.015 \times R_{0.01}}, \quad (6)$$

where $A_{0.01}$ denotes the path attenuation due to rainfall exceeding 0.01% of the time per year and $R_{0.01}$ is the rain rate exceeding 0.01% of the time per year expressed in mm/hr. The frequency and polarization dependent coefficients, a and b, can be found in ITU-R 838 [23]. Here, d represents the path length, and $r_{0.01}$ indicates the effective path length reduction factor when the non-uniform nature of rain, path length (d), and the rainfall intensity of $R_{0.01}$ are taken into account. While $R_{0.01}$ is less than 100 mm/hr, d_0 should be computed by the real rainfall value exceeding 0.01% of the time per year. While $R_{0.01}$ is greater than 100 mm/hr, d_0 should be computed by $R_{0.01}$=100 mm/hr. The procedure of rain attenuation prediction described here is suitable for all parts of the world. Once $A_{0.01}$ is obtained, ITU-R P.530 also provides a procedure for predicting fading for other percentages of the time per year [22]. In this paper, the LMDS system is assumed to operate at 28.35 GHz with vertical polarization. In the following analyses, rain attenuation is integrated into the calculation of intercell interference.

Due to the need for large data services, LMDS systems require high bandwidth efficiency to guarantee a specific bit error rate (BER) for the corresponding channel condition. A higher order modulation scheme can increase the throughput (bits/symbol) to, for example, 6 bits/symbol for 64 QAM modulation, but it is ineffective for low SINRs [22]. To maximize throughput, the appropriate modulation can be assigned to a given partial area of a cell according to the SINR and the relative SINR thresholds ($\mathrm{SINR_{th}}$). This is referred to as *dynamic modulation* [24]. When the values of key parameters vary, the SINR value varies accordingly; therefore, another modulation scheme can be adopted. To guarantee the corresponding capacity, the hierarchical modulation is considered to cover a specific coverage issue. QPSK, 16 QAM, and 64 QAM are considered for different bandwidth efficiencies and SINR thresholds. For example, given a BER of 10^{-6}, the values of the system $\mathrm{SINR_{th}}$ are 12.3 dB, 19.2 dB, and 25.5 dB for QPSK, 16 QAM, and 64 QAM, respectively. The performance criterion is based on area coverage ratio, which is expressed as a ratio of the sector area where the received SINR exceeds the SINR thresholds. The coverage ratio is defined by

$$\text{Coverage ratio} \equiv \frac{\text{Area of } (\mathrm{SINR} \geq \mathrm{SINR_{th}})}{\text{Sector area}}. \quad (7)$$

Furthermore, a spreading factor of $4 \cdot N = 4 \cdot 64 = 256$ under $\mathrm{BER} = 10^{-6}$ condition, the TS antenna with a beamwidth of 5° [5], and $D = 5$ km are taken to implement the simulation. Figures 2 to 4 demonstrate that the coverage ratios vary with the significant factors, namely, the rain rate and the number of users in each sector where the system is operating with DBPC.

Figure 2 shows that, in general, the coverage ratios of the three modulation schemes decrease as the rain rates increase under fully loaded conditions ($K_{sec} = 64$), except for some light rain rates. This is mainly because rain drops obstruct the intercell interference coming from the interfering BSs; hence, the performance of LMDS systems under drizzle conditions is better than under clear sky conditions. On the other hand, as a result of the rain drops simultaneously obstructing the desired signals and the intercell interference, the coverage ratio for QPSK, 16 QAM, and 64 QAM rapidly deteriorate as the rain rates increase to more than than 35 mm/hr, 25 mm/hr, and 20 mm/hr, respectively. Obviously, QPSK has the best coverage ratio of the three modulation schemes and 64 QAM is the most sensitive.

Figure 3 shows that in general the coverage ratios of the three modulation schemes decrease as the value of K_{sec} increases under clear sky conditions. The coverage ratios of QPSK slightly vary with the value of K_{sec}. Nevertheless, the coverage ratio for 64 QAM dramatically decreases as the value of K_{sec} increases.

Figure 4 shows that the coverage ratios for various rain rates vary with the value of K_{sec}. Obviously, the coverage ratios decrease as the value of K_{sec} increases whenever the rain rate is zero. As a result, the intercell interference increases as the value of K_{sec} increases. However, the coverage ratios have a tendency

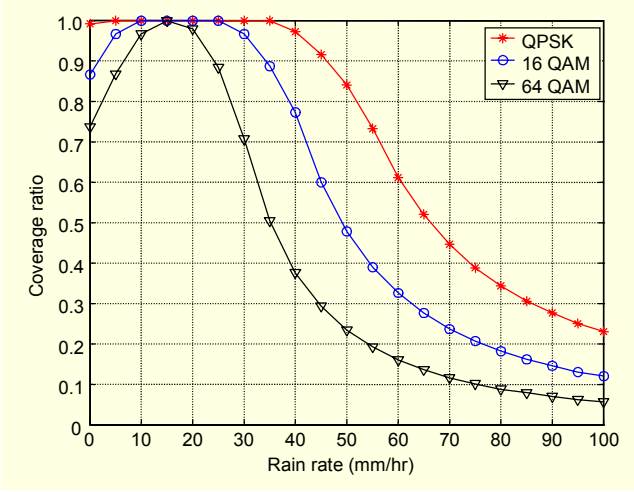

Fig. 2. Coverage ratios for OPSK, 16 QAM, and 64 QAM on various rain rates (BER = 10^{-6}, K_{sec} = 64, D = 5 km).

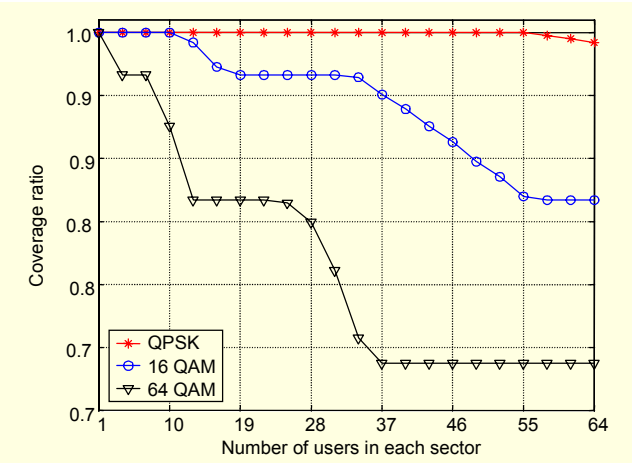

Fig. 3. Coverage ratios for OPSK, 16 QAM, and 64 QAM vary with number of users in each sector (BER = 10^{-6}, rain rate = 0, D = 5 km).

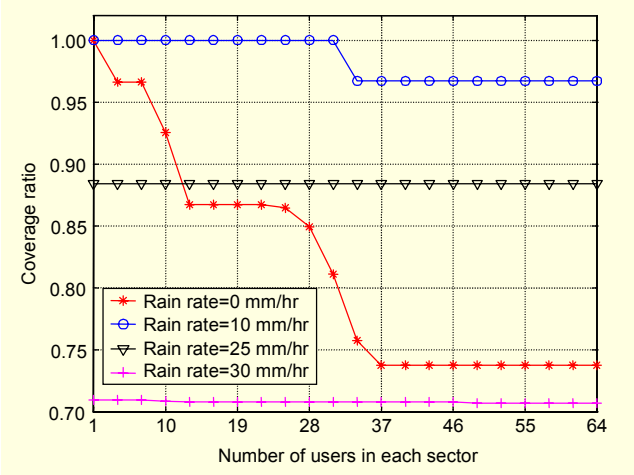

Fig. 4. Coverage ratios for the various rain rates vary with numbers of users in each sector ($SINR_{th}$ = 25.5 dB, D = 5 km).

toward stabilization when the rain rate is greater than 10 mm/hr, and the influence of the value of K_{sec} on the coverage ratio is insignificant under rainy conditions. Under light rain conditions (about 10 mm/hr), the intercell interference is blocked by rain drops. However, rain drops simultaneously obstruct the desired signals and intercell interference, resulting in a decrease in the coverage ratio when the rain rate is greater than 10 mm/hr. Comparison of Fig. 2 with Fig. 4 demonstrates that the influence of the rain rate on the coverage ratio is greater than the influence of K_{sec}.

III. Adaptive Neuro-Fuzzy Inference System

The concept of ANFIS is explained in this section. It is applied to the power control scheme for downlink CDMA-based LMDS systems. Further details of ANFIS can be found in [20]. The ANFIS scheme combines neural networks with the fuzzy inference system (FIS), and this has the advantages of easy implementation and learning ability. The FIS can store the essential components in the rule base and database and then infer the overall output values by applying human knowledge and fuzzy reasoning. That is, the FIS simulates the behavior of given if-then rules through knowledge of experts or an available database of the system. Neural networks have a significant learning ability, by which a desired input-output mapping can be obtained through a set of learning rule and training data. In ANFIS, the FIS is put into a five-layer adaptive network. The hybrid learning rule, which combines a back-propagation type gradient descent and the least-square estimate, is used to optimize the parameters of fuzzy inference systems on an adaptive network. In other words, the main objective of ANFIS is to identify the near-optimal membership functions and other parameters of the equivalent FIS by applying a hybrid learning algorithm using input-output data sets, and then to achieve a desired input-output mapping. ANFIS can approximate all nonlinear systems using less training data, a speedy learning process, and superior precision.

For simplicity, assume that the fuzzy inference system has two inputs, x and y, one output dq. The rule base contains two fuzzy if-then rules for Takagi and Sugeno's (T-S) fuzzy model which are expressed as follows:

$$\text{If } x \text{ is } A_1 \text{ and } y \text{ is } B_1, \text{ then } q_1 = f_1 x + g_1 y + h_1.$$
$$\text{If } x \text{ is } A_2 \text{ and } y \text{ is } B_2, \text{ then } q_2 = f_2 x + g_2 y + h_2.$$

Here, "x is A_1 and y is B_1" and "x is A_2 and y is B_2" are called the premise section, while "$q_1 = f_1 x + g_1 y + h_1$" and "$q_2 = f_2 x + g_2 y + h_2$" are called the consequent section. The corresponding equivalent ANFIS architecture shown in Fig. 5 is a class of adaptive networks which are functionally equivalent to FIS. ANFIS is a multilayer feed-forward

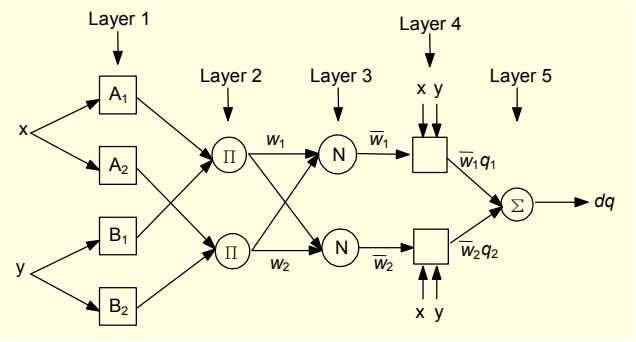

Fig. 5. Architecture of ANFIS.

network in which each node carries out a special task on incoming signals and a set of parameters relating to this node. The characters of the node function may vary from node to node, and the choice of node function depends on the overall input-output function of the adaptive network.

In Fig. 5, each node is represented by a square or a circle, reflecting the different adaptive capabilities of the nodes. The square nodes with parameters are adaptive nodes, whereas the circular nodes are fixed without any parameters.

In layer 1, each node is an adaptive node with the function of computing the degree of membership functions of each input. As shown in Fig. 5, x and y are the inputs of nodes, and A_i and B_i (i=1, 2,···) are the linguistic labels (large, small, and so on), associated with the node functions. The outputs of the nodes are the membership functions which denote the degrees to which the given inputs satisfy either quantifier A_i or B_i. The number of nodes represents the number of fuzzy sets. In this work, bell-shaped membership functions are chosen for this layer. All membership functions take on the values of the interval [0, 1] and are expressed as

$$\mu_{A_i}(x) = \frac{1}{1+\left|\frac{x-c_i}{a_i}\right|^{b_i}}, \quad i = 1, 2, \tag{8}$$

where $\{a_i, b_i, c_i\}$ is the *premise parameter set*. Function $\mu_{A_i}(x)$ or $\mu_{B_i}(y)$ is the bell-shaped function, which varies are the values of these parameters vary, consequently exhibiting various forms of membership functions on linguistic labels. In other words, the parameters a_i, b_i, and c_i are used to determine the shape and the position of the bell-shaped membership function. That is, the values of a_i and c_i can be used to adjust the width and the center of membership function. The value of b_i is usually greater than 0 and the values of b_i and a_i are employed to control the slopes at the intersecting point. The a_i, b_i, and c_i values can be determined during the training process of the hybrid learning algorithm.

Layers 2 and 3 have fixed nodes, which have no parameters. The nodes of these two layers are labeled Π or N, respectively. The nodes of layer 2, which implement the multiplication (or *t*-norm) operation of fuzzy sets, multiply the incoming signals by a scaling factor and send the outputs to the nodes of layer 3. The outputs of the nodes (w_i) are applied to represent the firing strength of each rule, and is defined as

$$w_i = \mu_{A_i}(x) \times \mu_{B_i}(y), \quad i = 1, 2. \tag{9}$$

In layer 3, each node normalizes the firing strength of each rule. The outputs of layer 3 are called *normalized firing strengths* and are fed forward to layer 4. Each node calculates the ratio of the firing strength of each rule to the sum of all firing strengths of the rules:

$$\overline{w}_i = \left(\frac{w_i}{\sum_i w_i}\right), \quad i = 1, 2. \tag{10}$$

Each node in layer 4 is an adaptive node with the function of making a simple linear combination from the system inputs and a set of parameters to the outputs of layer 3, and then calculating the contribution of each rule toward the overall output:

$$\overline{w}_i \times q_i = \overline{w}_i \times (f_i x + g_i y + h_i), \tag{11}$$

where $\{f_i, g_i, h_i\}$ is the *consequent parameter set*, q_i denotes the output of the rules, and $\overline{w}_i$ is the output of layer 3. The f_i, g_i, and h_i values can be determined by the training process of the hybrid learning algorithm.

In layer 5, a single node is a fixed node labeled Σ, which calculates the overall outputs to obtain the system output by summation of all incoming signals. The output is the weight sum of the results of the rules and is expressed as

$$dq = \sum_i \overline{w}_i q_i, \quad i = 1, 2. \tag{12}$$

These layers represent the equivalent of the T-S type fuzzy if-then rules. ANFIS integrates a fuzzy inference engine with an adaptive network, which learns the relationship between inputs and outputs.

Figure 6 illustrates the fuzzy reasoning mechanism for a two-rule two-input ANFIS scheme, which is divided into two sections, namely, a premise section and a consequent section. The output of each rule is a linear combination of the input variables and the constant terms. The total output is the weighted average of each rule output. The premise section performs the fuzzification of the input variables and then obtains the membership value. The membership value of the premise section is combined to obtain the weight of each rule by means of multiplication (or a *t*-norm operation). In the consequent section, the weighted value of each rule is used to generate the qualified consequent of each rule. The overall

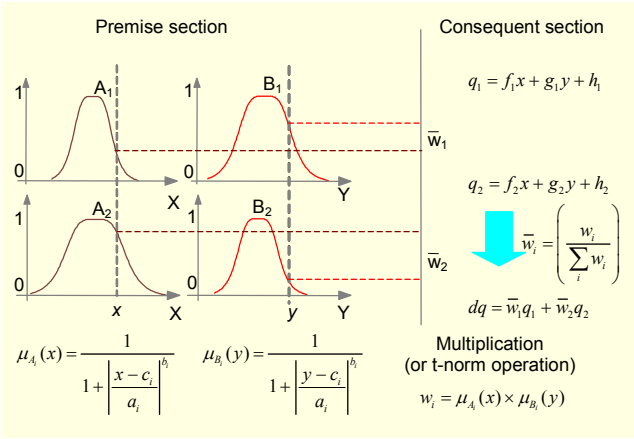

Fig. 6. FIS of ANFIS scheme.

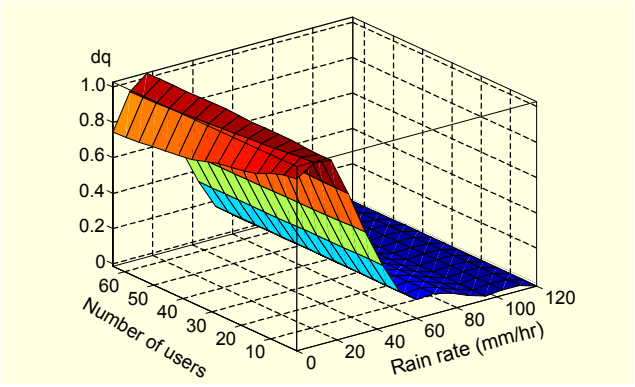

Fig. 7. Input-output mapping of ANFIS.

output is obtained by the summation of all results of the output. As shown in Fig. 5, given the value of premise parameters, the overall output (dq) can be expressed as the linear combination of the consequent parameters; therefore, (12) can be rewritten as

$$\begin{aligned} dq &= \bar{w}_1 q_1 + \bar{w}_2 q_2 \\ &= \bar{w}_1 (f_1 x + g_1 y + h_1) + \bar{w}_2 (f_2 x + g_2 y + h_2). \end{aligned} \tag{13}$$

Obviously, (13) is a linear parameter function so the well known linear least-square method can be applied to identify the linear parameters. To overcome the chief disadvantages of the adaptive network (slowness and tendency to become trapped in local minima), ANFIS employs hybrid learning rules, which combine the gradient method with a linear least-square method to take the place of the gradient descent method, and the hybrid learning method is applied to adaptive networks. Each epoch of the hybrid learning rule consists of a forward pass and a backward pass. The parameters can be partitioned into two subsets, a premise parameter and a consequent parameter. In the forward pass, input data is provided to each node. Functional signals go forward to calculate each node output layer by layer until layer 4. The consequent parameters f_i, g_i, and h_i are identified by the least-square estimate. This process is repeated for all the training data entries and the error measurement is obtained. In the backward pass, the error rates, which are derived from the error measurement, propagate backward from the output end to the input end, and the premise parameters a_i, b_i, and c_i are updated by gradient descent after the backward pass.

The hybrid learning rules not only decrease the dimension of the search space in the gradient method, but also accelerate convergence. In other words, it can speed up the training process, and it is more accurate and efficient than the conventional gradient decent scheme.

IV. ANFIS-Based Power Control

In this study, the coverage ratios for DBPC, which vary with the rain rate and the number of users in each sector (K_{sec}), are employed in the hybrid learning rules to generate the training database. This training procedure is needed only once.

The proposed scheme employs a batch of inputs and then outputs the quality of channel, which is used to adjust the radius of the power control region. Because the training and learning procedure is needed only one time, it can be done offline; thus, the computational complexity can be reduced. The ANFIS converts the fuzzy inference engine into an adaptive network that learns the relationship between the inputs and the outputs. Selecting an appropriate number of membership functions is essential for improving the convergence speed of the ANFIS algorithm. For our simulation, the number of membership functions for each input variable is determined by a trial and error process for simplicity. The rain rate and the number of users in each sector are the two system input parameters, and four linguistic variables for each input parameter are used to obtain the desired performance. Here, the ANFIS contains 16 fuzzy rules, and the total number of parameters is 72, including both 24 premise parameters and 48 consequent parameters. A total of 7,744 training data pairs are obtained and stored along with the corresponding operating conditions. We apply the stored data to train the ANFIS algorithm. The ANFIS input-output mapping is plotted in Fig. 7, which shows the relationship between the two inputs (rain rate and K_{sec}) and one output (dq). The output of ANFIS is channel quality, which is denoted by dq. The value of dq must be within in the interval [0, 1].

In the downlink power control model, we assume that when the location of the i-th TS is known, the power required to reach the i-th TS can be adjusted and expressed as

$$P(r_i) = F_i \times P_D, \quad 0 \le F_i \le 1, \tag{14}$$

where r_i is the distance between the desired BS and the i-th TS,

F_i denotes the power control factor, and P_D is the power required to reach the TSs which are located at the boundary area (BA) as shown in Fig. 1.

The DBPC scheme [14]-[16] applies the distance between the desired BS and TS to allocate the transmitted power to each of its served TSs. It is an open-loop power control scheme, meaning that the transmitted power is computed directly, and there is no feedback or correction supplied to the desired BS. In DBPC, the power control factor (F_i) is given by

$$F_i = \begin{cases} 1, & r_i \geq D, \\ (r_i/D)^2, & 0 < r_i \leq D, \end{cases} \tag{15}$$

where D is the distance from the desired BS to the cell boundary as shown in Fig. 1. When $0 < r_i \leq D$, that is, when the TS is located within the power control region, the BS adopts $F_i = (r_i/D)^2$ to allocate the transmitted power to the i-th TS. Therefore, the power required to reach the TS merely depends on the distance between the desired BS and the i-th TS. When r_i is greater than D, that is, when the i-th TS is located at the boundary area, the BS adopts F_i=1 to allocate the transmitted power to the i-th TS. LMDS is a fixed broadband wireless access system. The subscriber is fixed, and the DBPC is carried out once after the distance data of the TSs is obtained.

Accordingly, this work proposes ANFIS power control, which adjusts the radius of power control region according to the channel quality (dq). In this proposed ANFIS power control, the power control factor (F_i) is expressed as

$$F_i = \begin{cases} 1, & r_i > L_{\text{thr}}, \\ (r_i/D)^2, & 0 < r_i \leq L_{\text{thr}}, \end{cases} \tag{16}$$

where L_{thr} is both the threshold distance and the radius of the power control region. Note that L_{thr} is derived from dq and is defined as

$$L_{\text{thr}} = dq \times D. \tag{17}$$

When $0 < r_i \leq L_{\text{thr}}$, that is, when the i-th TS is located within the power control region, the BS adopts $F_i = (r_i/D)^2$ to allocate the transmitted power to the i-th TS. The transmitted power varies with the distance between the desired BS and the i-th TS. In contrast, when $r_i > L_{\text{thr}}$, that is, when the i-th TS is located outside the power control region, the BS adopts F_i=1 to allocate the transmitted power to the i-th TS. That is, the BS allocates P_D transmitted power to the TSs which are located in this area. Accordingly, a smaller value of dq implies that the system has lower channel quality, and this leads to a smaller power control region. Consequently the required power for most of the TSs is P_D, and this results in a higher total power consumption. In contrast, a higher value of dq implies that the system has higher channel quality, and this leads to a larger power control region. Consequently, the required power for most of the TSs is $P(r_i)$, which is less than P_D, resulting in a lower total power consumption. In other words, a smaller power control region results from lower channel quality, and the transmitted power allocated to most TSs is P_D. On the other hand, a larger power control region results from higher channel quality where most TSs located within the power control region, and the power required varies with the distance. In the proposed ANFIS power control, the BS allocates the transmitted power to the TS on the basis of channel quality rather than only on the basis of distance. Accordingly, the proposed ANFIS power control can compensate for the attenuations caused not only by path loss and intercell interference but also by weather conditions and intercell interference.

The detailed operation of the ANFIS-based power control can be summarized in the following steps.

Step 1. Input the parameters of the system, the rain rate data, and the number of users in each sector to implement the DBPC scheme and then to output the training database.

Step 2. Apply the training database, the input data, and the operation conditions to construct the ANFIS structure.

Step 3. Acquire real-time meteorological forecast data from the weather bureau. Based on the MAC protocol used, the BS acquires the number of users in each interfering sector, and then these two sets of data are used as input of the ANFIS-based power control scheme to predict the channel quality (dq).

Step 4. The value of dq is applied to determine the threshold distance, which is used to calculate the power control region.

Step 5. The BS adjusts the transmission power for each individual TS based on the power control region and the TS locations. This can guarantee that the communication is available under the given weather conditions.

Step 6. Repeat steps 3 to 5. Note that the update frequency is based on the local weather bureau forecast time.

For ease of comparison, assume that all the BSs adopt the same power control scheme and that there are N users uniformly distributed in a sector. Before the calculation of the power reduction function (Q) for a power control scheme, the user density (ρ) in a sector should be defined as

$$\rho = N/D^2. \tag{18}$$

Using downlink power control, the total transmitted power of the BS allocated to all the TSs within a given sector are computed as

$$\begin{aligned} P_T &= \iint_A P(r) \times \rho \, dA \\ &= \iint_{A_1} P(r) \times \rho \, dA + \iint_{A_2} P_D \times \rho \, dA, \end{aligned} \tag{19}$$

where $P(r)$ is obtained from (14), A_1 and A_2 are the power

control region and the other zone within the given sector, respectively. Suppose that in the case of no power control P_D is needed by all users in the sector. The total transmitted power for all users in the sector can be expressed as

$$P_T = N \times P_D. \tag{20}$$

The power reduction function (Q) is defined as the ratio of the scheme with power control scheme (19) to the scheme without power control, that is, (20). This can be expressed as

$$\begin{aligned} Q &= \sum F_i / N \\ &= \left[\iint_{A_1} (r/D)^2 \times \rho dA + \iint_{A_2} 1 \times \rho dA \right] / N. \end{aligned} \tag{21}$$

Suppose that all BSs adopt the same power control scheme in our simulation due to implementation of the downlink power control. The desired signal strength and the interfering signal strength will be reduced F_i and Q times, respectively.

In practice, this system can adopt the weather forecast data provided by the weather bureau to predict the average rain rate as well. LMDS is a two-way PMP system, where different BSs can exchange information with each other through upper layer communications; thus, the rain rate and number of users in each sector (K_{sec}) can be determined. The proposed ANFIS power control can be updated whenever data is available.

As mentioned in section II, different modulation schemes are assigned to partial areas within a cell sector to maximize the throughput according to the SINR and the relative $SINR_{th}$. Dynamic modulation and power control schemes are applied to the downlink CDMA-based LMDS systems to improve the average throughput and to increase the system capacity. Here, the average throughput (bits/symbol) for dynamic modulation can be calculated as

$$\text{Average throughput} = \frac{S_1 \times 2 + S_2 \times 4 + S_3 \times 6}{\text{Sector area}}, \tag{22}$$

where S_1, S_2, and S_3 are three partial areas in which QPSK, 16 QAM, and 64 QAM modulations are respectively adopted within the given sector. Since the subscribers in LMDS networks are fixed, the system design must cover the worst case; otherwise, some TSs will not satisfy the QoS requirements. As shown in Fig. 1, by considering the upper-right corner sector of BS0 with vertical polarization, a spreading factor of $4N = 256$, $D = 5$ km, dynamic modulation under BER = 10^{-6}, and fully loaded ($K_{sec} = N = 64$), the DBPC and proposed ANFIS power control schemes were implemented. The simulation results shown in Fig. 8 demonstrate that heavier rain rates lead to lower average throughput, and that the average throughput of ANFIS power control is always higher than that of DBPC power control schemes. On clear sky and slightly rainy conditions, that is, when the rain rate is less than 30 mm/hr, the throughput of two power control schemes is about the same; however, the ANFIS scheme always has slightly higher throughput when the rain rate is higher than 30 mm/hr.

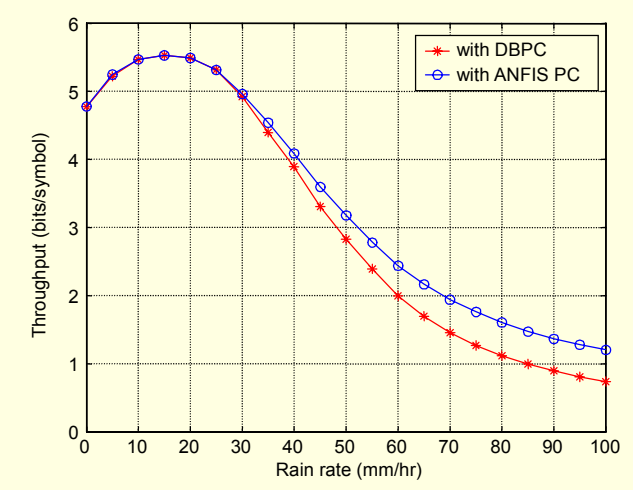

Fig. 8. Average throughput with DBPC and ANFIS power control at various rain rates (dynamic modulation with BER = 10^{-6}, $K_{sec} = 64$, $D = 5$ km).

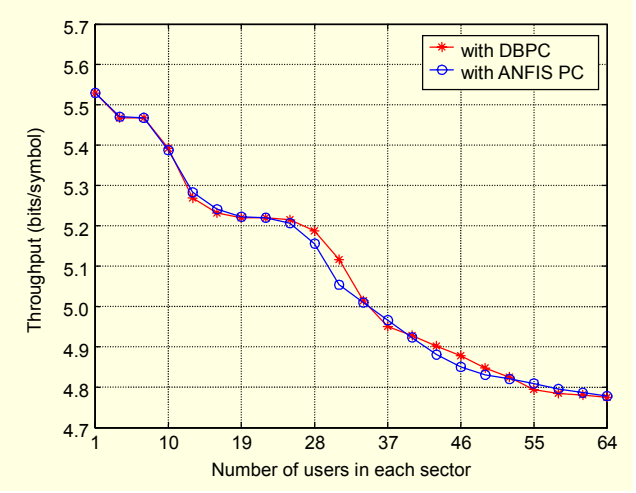

Fig. 9. Average throughput with DBPC and ANFIS power control with various numbers of users in each sector (dynamic modulation with BER = 10^{-6}, rain rate = 0, $D = 5$ km).

Figure 9 demonstrates that, in general, the average throughput decreases as the value of K_{sec} increases when the system is operated under the conditions in Fig. 8; however, the value of K_{sec} varies from 1 to 64 under clear sky conditions (rain rate = 0). Under the conditions in Fig. 9, ANFIS power control and DBPC perform equally well. However, considering both Figs. 8 and 9, the proposed ANFIS power control provides better average throughput under rainy condition than DBPC without affecting the average throughput under clear sky conditions.

V. Conclusion

In this paper, the application of ANFIS power control to enhance the performance of downlink CDMA-based LMDS systems has been investigated thoroughly with a system model, intercell interference, and rain attenuation influences being considered. Rain attenuation and intercell interference severely affect the performance of LMDS which operates above 20 GHz. The DBPC scheme improves the performance of downlink CDMA-based LMDS systems by reducing the intercell interference under clear sky conditions, but it may damage the performance of downlink CDMA-based LMDS systems under rainy conditions. Consequently, the proposed ANFIS power control adjusts the radius of power the control region on the basis of channel quality rather than on the basis of the distance alone. Hence, the system can work robustly under both clear sky and rainy conditions. Simulation results show that the average throughput and dynamic modulation of the proposed ANFIS power control are superior to those of DBPC schemes.

Acknowledgment

The authors would like to thank the anonymous reviewers for their valuable comments on this paper.

Reference

[1] H. Sari, "Broadband Radio Access to Homes and Businesses: MMDS and LMDS," *Comput. Netw.,* vol. 31, 1999, pp. 379-393.

[2] D.A. Gray, "A Broadband Wireless Access System at 28 GHz," *Proc. NIST–Cosponsored Conf. on Wirel. Commun.,* Boulder, CO, 11-13 Aug. 1997, pp. 1-7.

[3] S.Q. Gong and D. Falconer, "Cochannel Interference in Cellular Fixed Broadband Access Systems with Directional Antennas," *Wirel. Pers. Commun*., vol. 10, no. 1, June 1999, pp. 103-117.

[4] C. Novák, A. Tikk, and J. Bitó, "Code Sectoring Methods in CDMA-Based Broadband Point-to-Multipoint Networks," *IEEE Microwave and Wireless Components Letters*, vol. 13, 2003, pp. 320-322.

[5] P.D.M. Arapoglou et al., "Intercell Radio Interference Studies in CDMA-Based LMDS Networks," *IEEE Trans. Anten. & Propag.*, vol. 53, no. 8, Aug. 2005, pp. 2471-2479.

[6] A.D. Panagopoulos et al., "Intercell Radio Interference Studies in Broadband Wireless Access Networks," *IEEE Trans. Veh. Technol.*, vol. 56, no. 1, Jan. 2007, pp. 3-12.

[7] M.K. Tsay and F.T. Wang, "Cellular Architecture on CDMA-Based LMDS," *Proc. Third Int. Symp. CSNDSP*, Staffordshire, U.K., July 2002.

[8] C.-Y. Chu and K.S. Chen, "Effects of Rain Fading on the Efficiency of the Ka-Band LMDS System in the Taiwan Area," *IEEE Trans. Veh. Technol.*, vol. 54, no. 1, Jan. 2005, pp. 9-19.

[9] H. Halbauer, P. Jaenecke, and H. Sari, "An Analysis of Code-Division Multiple Access for LMDS Networks," *Proc. 7th European Conf. Fixed Radio Systems and Networks*, Dresden, Sept. 2003, pp. 173-180.

[10] H. Sari, "A Multimode CDMA with Reduced Intercell Interference for Broadband Wireless Networks," *IEEE J. Select. Areas Commun*., vol. 19, no. 7, July 2001, pp. 1316-1323.

[11] C. Sinka and J. Bitó, "Site Diversity against Rain Fading in LMDS systems," *IEEE Microw. Wireless Compon. Lett.*, vol. 13, no. 8, Aug. 2003, pp. 317-319.

[12] A.D. Panagopoulos, V.K. Katsambas, and J.D. Kanellopoulos, "A Simple Model for Differential Rain Attenuation Statistics on Converging Terrestrial Microwave Paths," *IEEE Antennas Wireless Propag. Lett.*, vol. 2, 2003, pp. 82-85.

[13] Y.M. Siu and K.K. Soo, "CDMA Mobile Systems with Tailor Made Power Control to Each Mobile Station," *Proc. in IEE 1st. Int. Conf. on 3G Mobile Commun. Tech.*, no. 471, Mar. 2000, pp. 46-50.

[14] W.C.Y. Lee, "Overview of Cellular CDMA," *IEEE Trans. Veh. Technol.*, vol. 40, no. 2, May 1991, pp. 291-302.

[15] R.R. Gejji, "Forward-Link-Power Control in CDMA Cellular Systems," *IEEE Trans. Veh. Technol.*, vol. 41, no. 4, Nov. 1992, pp. 532-536.

[16] L. Nuaymi, P. Godlewski, and X. Lagrange, "Power Allocation and Control for the Downlink in Cellular CDMA Networks," *Proc. 12th IEEE Int. Symp. PIMRC,* vol. 1, San Diego, 2001, pp. c-29–c-31.

[17] P.R. Chang and B.C. Wang, "Adaptive Fuzzy Power Control for CDMA Mobile Radio Systems," *IEEE Trans. Veh. Technol.*, vol. 45, no. 2, May 1996, pp. 225-236.

[18] X. Wu, L. Ge, and G. Liang, "Adaptive Power Control on the Reverse Link for CDMA Cellular System," *Proc. IEEE 15th APCC / OECC '99 Commun*., vol. 1, Oct. 1999, pp. 608-611.

[19] M.K. Tsay, Z.S. Lee, and C.H. Liao, "Fuzzy Power Control for Downlink CDMA-Based LMDS Network," *IEEE Trans. Veh. Technol.*, vol. 57, no. 6, Nov. 2008, pp. 3917-3921.

[20] J.S.R. Jang, "ANFIS: Adaptive-Network-Based Fuzzy Inference Systems," *IEEE Trans. Syst. Man and Cybern.*, vol. 23, no. 3, 1993, pp. 665-685.

[21] E.H. Dinan and B. Jabbari, "Spreading Codes for Direct Sequence CDMA and Wideband CDMA Cellular Networks," *IEEE Commun. Mag.*, vol. 36, Sept. 1998, pp. 48-54.

[22] ITU-R, *Propagation Data and Prediction Methods Required for the Design of Terrestrial Line-of-Sight Systems*, ITU-R Rec. P530–10, 2001.

[23] ITU-R, *Specific Attenuation Model for Rain for Use in Prediction Methods,* ITU-R Rec. P838-2, 2003.

[24] C.H. Lee, B.Y. Chung, and S.H. Lee, "Dynamic Modulation

Scheme in Consideration of Cell Interference for LMDS," *Proc. Int. Conf. Commun. Tech.*, vol. 2, Beijing, China, Oct. 1998, pp. S38-8-1-S38-8-5.

Ze-Shin Lee received the MS degree in computer science and electrical engineering from Yuan-Ze Institute of Technology (YZIT, Taiwan) in 1994, and the PhD degree in communication engineering from the National Central University (NCU) of Taiwan in 2008. He is an instructor with the Department of Electrical Engineering, Minghsin University of Science and Technology (MUST), Taiwan. His research interests are in the areas of wireless communications systems and digital signal processing.

Mu-King Tsay received his BS degree from the National Cheng-Kung University (NCKU, Taiwan) in 1969 and his MS degree from the National Central University (NCU, Taiwan) in 1972. He was a visiting expert for two years in the field of remote sensing at NOAA, Boulder, CO, from 1979 to 1981. He was also an associate professor with the Institute of Computer Science and Electrical Engineering and a professor with the Institute of Electrical Engineering of NCU, from 1981 to 2003. He has been a professor with the Department of Communication Engineering of NCU since 2003. His current research interests include communications systems, remote sensing, data compression, signal processing, and pattern recognition.

Chien-Hsing Liao received his MS degree in telecommunication engineering from the National Chiao-Tung University (NCTU, Taiwan) in 1991, and the PhD degree in communication engineering from the National Central University (NCU) of Taiwan in 2008. He is a senior SATCOM communications engineer with Chung-Shan Institute of Science and Technology (CSIST), Taiwan. His current research interests are in the area of secure wireless and satellite communications systems.